NRIAG JOURNAL OF ASTRONOMY AND GEOPHYSICS
2020, VOL. 9, NO. 1, 375–392
https://doi.org/10.1080/20909977.2020.1746893

Mineralogy and ground gamma-ray spectrometric investigation for phosphates of Gabal Abu Had area, Central Eastern Desert, Egypt

Ibrahim Gaafar[a], Mohamed Abu El Ghar[b], Tarek Ibrahim[a] and Mohamed Diab[a]

[a]Nuclear Materials Authority, Fayoum University, Al Fayyum, Egypt; [b]Faculty of Science, Fayoum University, Al Fayyum, Egypt

ABSTRACT

The present study deals with geologic and mineralogic studies as well as gamma-ray spectrometric survey for uranium potential phosphates of Duwi Formation and environmental assessment at Gabal Abu Had environ. These phosphate deposits are considered as an important potential resource for uranium and rare earth elements as by-products. The study area lies to the NE of Qena town and dissected by Qena – Safaga asphaltic road. The Duwi Formation in the study area conformably overlies Qusseir Formation and underlies Dakhla Formation; this succession is capped with Esna and Thebes Formations and eroded along wadis which are filled with Quaternary deposits. Phosphate deposits (Duwi Formation) of Abu Had area are enriched with uranium, which may be extracted as a by-product of making fertilisers. Petrographic studies indicate that phosphate beds are composed of phosphatic particles which include collophane grains, bioclasts (bone and teeth fragments), as well as, non-phosphatic particles which include quartz, calcite and pyrite embedded in silica, calcite or iron oxides cement. XRD results showed that hydroxylapatite is the principal phosphate mineral, and the non-phosphate minerals include calcite, quartz, gypsum and anhydrite. Ground gamma-ray spectrometric results indicated that the study area has K values range from 0.2% to 4.4%, eTh values range from 0.5 to 18 ppm and eU values range from 0.5 to 100 ppm. The phosphate-bearing beds of Duwi Formation have the highest values of eU reach up to 100 ppm. The uranium anomalies mostly elongated in NW-SE trend that related to the NW-SE strike-slip faults of the area. The average value of annual effective dose rates of phosphates at Abu Had area equals 0.32 mSv/y which, less than the worldwide permissible level of annual effective dose rate (1 mSv/y).

ARTICLE HISTORY
Received 10 December 2019
Revised 10 February 2020
Accepted 25 February 2020

KEYWORDS
Phosphate deposits; Duwi Formation; uranium anomalies; γ-ray spectrometric

1. Introduction

The Egyptian phosphate deposits are a part of the Middle East to North Africa phosphate province and confined to the Upper Cretaceous and Lower Tertiary sediments. The total resources of Egyptian phosphates estimated more than 3 billion tons (Notholt 1985). Gamma-ray spectrometric can be used for acquiring information on the distribution of radiation exposure rates (Gaafar et al. 2016). The phosphate occurrences in Egypt from north to south were subdivided into three east-west trending facies belts (Hermina 1972), that are northern, central and southern facies. The central facies belt represents the most economic occurrences and include three major localities, on the Red Sea Region, on both sides of the Nile Valley (east and west El Sibaiya area – Abu Had – Wadi Hamama) and Western Desert (Abu Tartur – Dakhla plateau). Many previous studies are made on the Nile Valley phosphorites and their uranium potentialities. For example, Morsery (1969), Philobbos (1969), El-Kammar (1970), Attia et al. (1971) McClellan (1980), Germann et al. (1984), Baioumy (2007), Zidan (2013), Abou El-Anwar et al. (2016) and Hassaan et al. (2017) concluded that collophane, bone and teeth fragments together with minor amounts of detrital quartz, carbonaceous, ferruginous material, pyrite, glauconite and shell fragments as the main constituents of the phosphorites at several localities along the Nile Valley. Ahmed (1983) analysed phosphate samples of collophane grains and bone fragments from Abu Had and Wadi Hamama area using XRD technique and pointed out that francolite has a similar composition in bone fragments and collophane grains, although it possesses a slightly higher Na and F contents in bone fragments. Mohamed (1994) reported that the known natural phosphorite minerals exceed 250 in number and they belong mostly to the apatite family.

The measured thickness of the Duwi Formation is about 105 m at Gabal Abu Had (Hamama and Kassab 1990). Abdu (2002) stated that the marine Nile Valley phosphate deposits are characterised by U-enrichment in their respect. Gaafar et al. (2014) integrate the airborne and carborne gamma-ray spectrometric surveys, Wadi El-Jidami area, Central Eastern Desert, Egypt, and mentioned that phosphatic rocks of Duwi Formation have a high content of uranium up to 42 ppm. Abbady (2004) estimates the radiological effects of sedimentary rocks from Upper Egypt in G. Sarai

CONTACT Ibrahim Gaafar gaafar_ibrahim@yahoo.com Nuclear Materials Authority, Fayoum University, Al Fayyum, Egypt

area and in G. Anz area and mentioned that the average absorbed dose rates are 0.16 mSv/y and 0.17 mSv/y for G. Anz and G. Sarai, respectively.

The airborne gamma-ray spectrometric survey is used in different fields. Mainly it is used in uranium exploration and geological mapping (Anderson and Nash 1997; IAEA 2010; Gaafar et al. 2017). It is also used in mineral exploration (Grasty and Shives 1997; Gaafar et al. 2013). It is also used in environmental radiation monitoring (Lahti et al. 2001; Ford et al. 2001). The data were gridded to producing colour contour maps for the three radioelement concentrations, and their ratios. The interpretation of these airborne spectrometric survey data will explain enrichment or depletion of these radioactive elements in different geological settings.

This paper deals with petrographical and mineralogical studies as well as ground gamma-ray spectrometric survey for uranium potential – phosphates of Gabal Abu Had environ, which lies to the NE of Qena town between Latitudes 26°20′00” and 26°32′30”N and longitudes 33°00′00” and 33°10′00”E. The studied area is dissected by Qena – Safaga Asphaltic road (Figure 1). However, the previous studies have limited results of airborne anomalies. Therefore, the present study applies the ground survey for follow-up of the airborne anomalies. The present study rings a large amount of new analytical data in a variety of speciality fields: geology, mineralogy, X-ray diffraction, geochemistry, interpretation of ground gamma spectrometry on an area hosting uranium mineralised phosphorites. This is an important subject because phosphates and uranium represent extremely valuable resources. The new finding of this study is the phosphate of Duwi Formation is enriched with U-minerals that reaching to 100 ppm and it is slightly less than the permissible level of annual effective dose rate.

2. Geological setting

The study area is composed mainly of a simple sedimentary succession ranges from Upper Cretaceous to Quaternary age (Figures 2–4). It characterised by the presence of Abu Had syncline with axial plane runs in (NW-SE) direction for about 40 km length, affected by the tectonic activity in the Gulf of Suez province and it is crossed by two main fault systems having (NW-SE) and (NE-SW) trends (El-Sawy et al. 2011). The Duwi Formation conformably overlies Qusseir Formation and conformably underlies the Dakhla Formation, Tarawan Formation and Esna Formation. This succession in the study area capped with Thebes Formation and eroded along wadis which are filled with Quaternary gravels, sands and shale. The following is

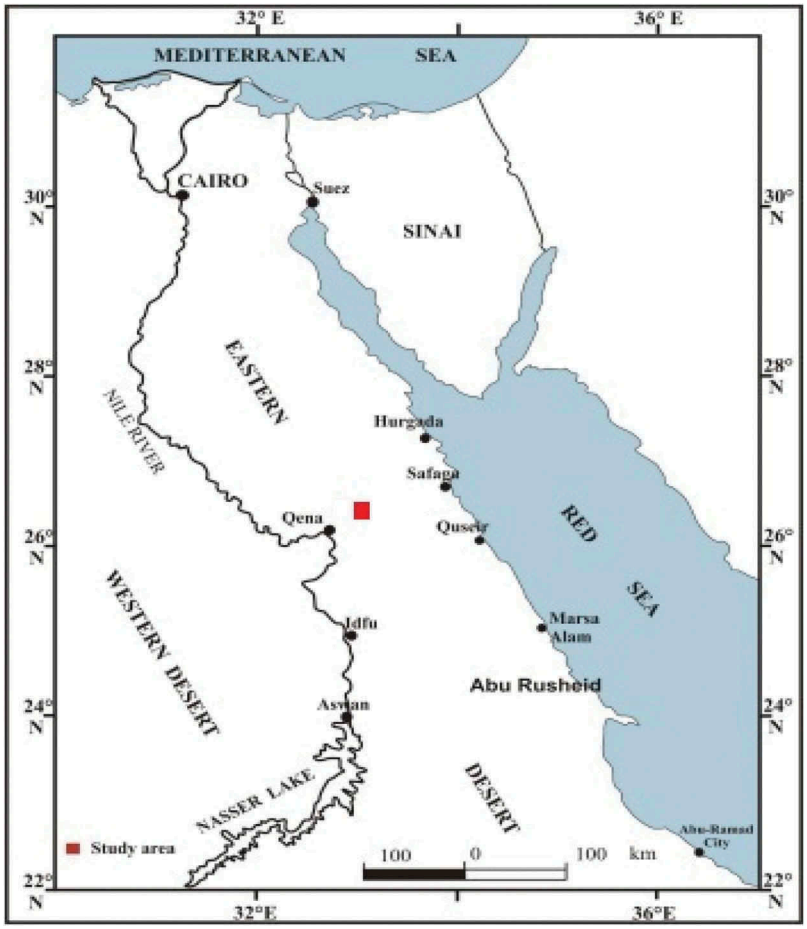

Figure 1. Location map of Abu Had area, Central Eastern Desert, Egypt.

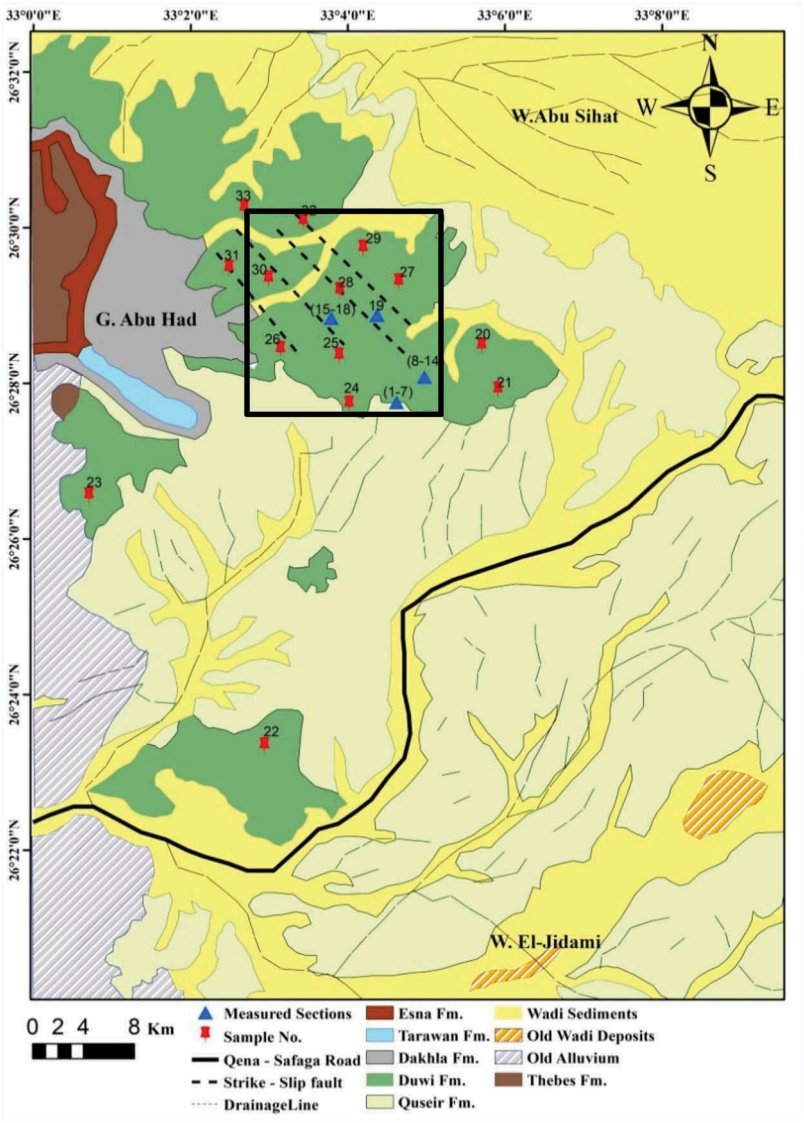

Figure 2. Geologic map of Abu Had area, Central Eastern Desert, Egypt (After EGSMA, 2001; 2002).

brief descriptions of the different formations exist in the study area from older to younger:

2.1. Qusseir formation

In the studied area this formation represented by variegated shale which conformably underlying the Duwi Formation and the contact between the Qusseir Formation and Duwi Formation is sharp as shown in (Figure 3(a)).

2.2. Duwi formation

The Duwi Formation in the study area conformably overlies the Qusseir Formation and underlying Dakhla Formation (Figures 3(a,d)). It represented by three phosphorite members where the lower member is composed of yellowish-brown phosphate bands at weathered exposed surface, interbedded with thin blackish shale, chert lenses and calcareous clay stone bed, the lower member ranges from 1.9 to 2.1 m in thickness with an average 2 m (Figure 3(a)). The middle member is composed of grey to black, papery shale, cross-bedded siltstone, marl, oyster bank and thin phosphatic layer. The shale has different colours being darker upwards; Iron bands often intercalated the shale, its maximum thickness approximately 57 m (Figure 3(b)). The upper member is composed of yellowish-brown phosphate at the weathered exposed surface with dolomitic lenses, black shale and capped with fossiliferous (ammonites) limestone bed, it ranges between 5.2 and 5.5 m in thickness with an average thickness of 5.35 m (Figure 3(c)).

2.3. Dakhla formation

Dakhla Formation overlies the Duwi Formation and underlies the Tarawan Formation. In the study area, Dakhla Formation exposed in Gabal Abu Had which lies in the north-western side of the study area. It consists of a series of marl and shale which vary in

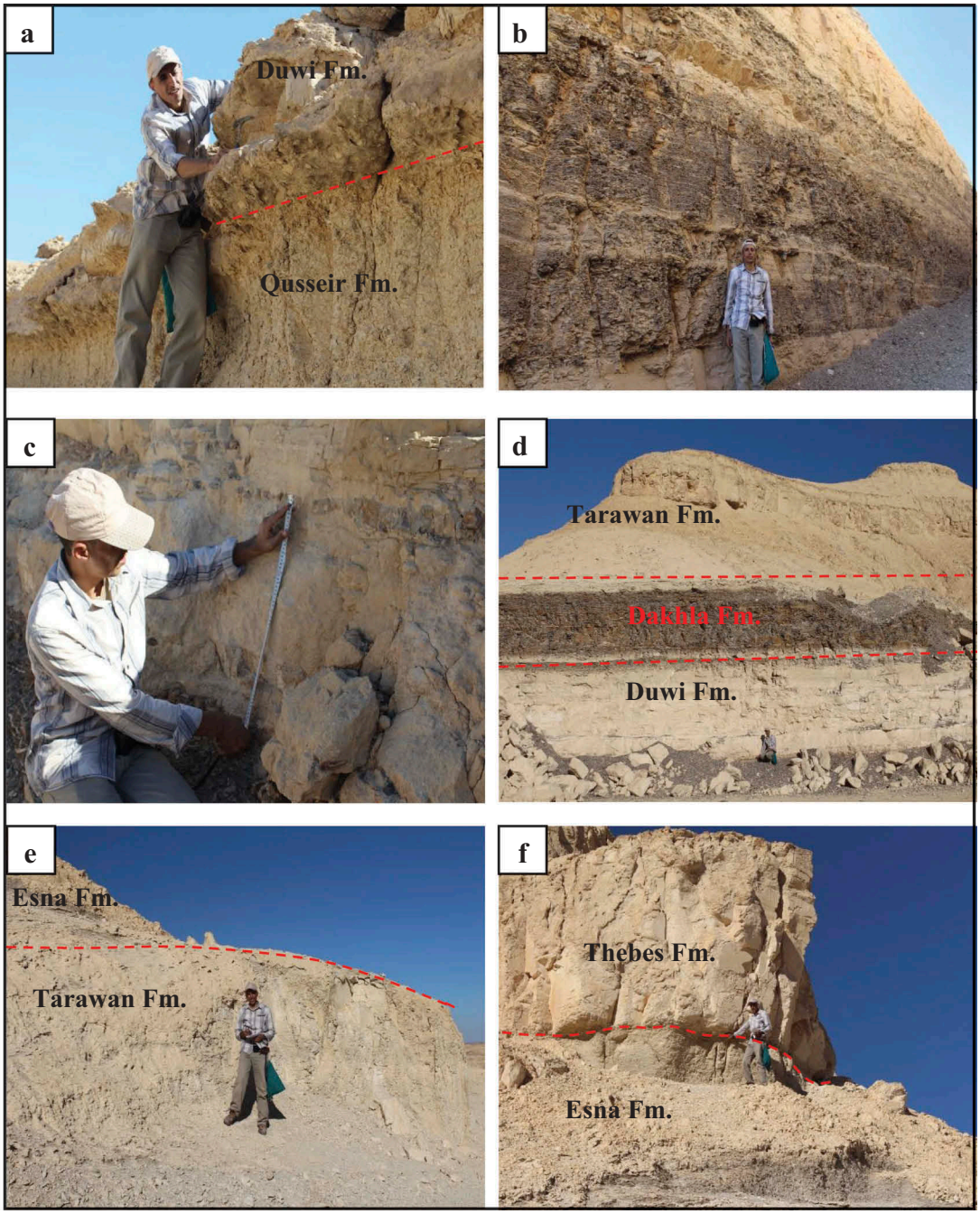

Figure 3. (a) The contact between Qusseir Formation and the lower member of Duwi Fm., (b) thickness of middle member of Duwi Fm., (c) thickness of upper member of Duwi Fm., (d) the contact between upper phosphate member of Duwi Fm., Dakhla Fm. and Tarawan Fm., (e) the contact between Tarawan Fm. and Esna Fm. and (f) the contact between Esna Fm. and Thebes Fm. in the study area.

thickness from one place to another and its thickness reaches 5 m in the study area (Figure 3(d)).

2.4. Tarawan formation

The Tarawan Formation is composed mainly of marl and marly limestone beds (Figure 3(e)). It is conformably underlined by the Dakhla Formation. The stratigraphic importance of Tarawan Formation comes from regarding it a marker between the Dakhla and Esna Formations. Its thickness reaches 9 m in the study area of Gabal Abu Had.

2.5. Esna formation

Esna Formation is recorded in the north-western side of the study area overlying the Tarawan Formation and underlying the limestone sequences of Thebes

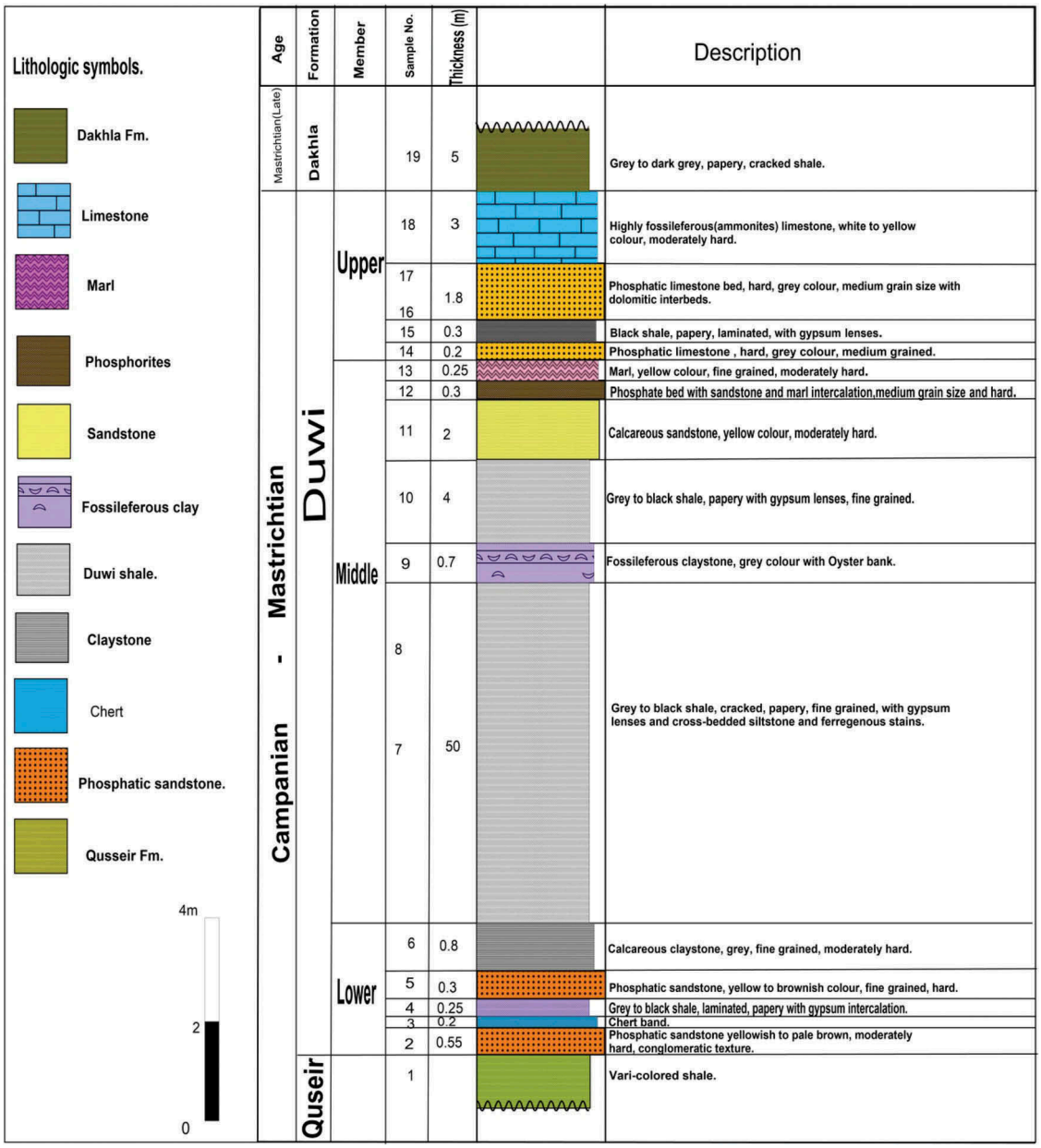

Figure 4. Composite lithostratigraphic section of Abu Had area, Central Eastern Desert, Egypt.

Formation. It composed of thick calcareous shale. The thickness of the Esna Formation increases southward to about 5 m at Abu Had study area (Figure 3(f)).

2.6. Thebes formation

The Thebes Formation overlies the Esna Formation and forms the north-western escarpment boundary of the Gabal Abu Had. Its thickness is more than 20 m in the study area (Figure 3(f)).

2.7. Quaternary deposits

Quaternary deposits in the study area are represented by the wadi fill deposits being composed mainly of conglomerate, sand and gravels. It represented by three sedimentary units, which are the Old Alluvium, Old Wadi deposits and Wadi sediments (Figure 2). It is distributed well in the study area, where they exposed in Wadi El-Jidami, Wadi Abu Sihat and Wadi El-Markh.

3. Methods of study

In the present study, 33 representative samples were collected and described from the beds. Twenty thin sections represented for phosphorites and phosphatic rocks of upper, middle and lower member of Duwi Formation of the study area were prepared and examined for the identification of the mineral constituents and texture by using a polarising microscope equipped with an automatic camera and a mechanical stage. The unknown minerals of phosphate rocks from the three members of Duwi Formation of the study area were prepared and investigated as bulk samples using the

X-ray diffraction technique (XRD) by PHILIPS PW 3710/31 diffractometer, scintillation counter; Cu-target tube and Ni filter at 40 kV and 30 mA to determine the mineralogical composition of phosphate. The mineralogical studies were carried out in the laboratories of the Egyptian Nuclear Materials Authority (NMA). Follow up of the airborne uranium anomalies for the northern part of the study area by ground gamma-ray spectrometric survey using RS-230 spectrometer, on a grid pattern with spacing 100 m with an increase of the grid stations to about 50 m spacing. The surface distribution of the eU, eTh, K and dose rate was determined, and image maps of these elements were constructed and interpreted.

4. Petrographical studies

Twenty thin sections of representative phosphate samples of studied area are composed of phosphate particles include mudclasts represented by peloids (collophane grains), bioclasts (bone and teeth fragments), beside non-phosphate particles of quartz, calcite and pyrite embedded in silica, calcite, iron oxides or gypsum cement.

4.1. Phosphate particles

Phosphatic mudclasts (collophane) were described as peloids by (El-Kammar et al. 1979) and occur in studied sections in sample 23 as yellow to brown colour. They are isotropic, showing spherical, oval, prismatic and irregular shapes (Figure 5(a)). The darker colours depend on the pigmentation of phosphatic grains by iron oxides. The size of collophane is ranging from silt to pebbly size.

Phosphatic bioclasts are recorded in samples 2, 22 and 25. They are represented mainly by brownish-yellow to yellow teeth and bone fragments ranging in size from medium, coarse to very coarse (up to 2 mm) grain. Teeth fragments of prismatic shape with grey to black colour and stained by iron oxides have been recorded in the studied phosphate samples (Figure 5 (b)). Bone fragments are present in different forms; subangular to rounded elongated forms (Figure 5(c)). They are characterised with grey to black colour which sometimes transformed into brownish red as a result of iron oxide staining. The planktonic Foraminifera sp. (Globgrinoid sp.) is present in uniserial and biserial forms in phosphate samples (Figure 5(d)). The abundance of planktonic Foraminifera in the studied section reflects a marine depositional environment of phosphates.

In the studied samples, the non-phosphate materials are represented by detrital quartz which recorded in samples 2, 12 and 20 (Figure 5(b)), calcite crystals in sample 20 (Figure 5(f)), pyrite crystals recorded in sample 12 (Figure 5(e)), and iron oxides present as replacement materials or filling matter of bioclasts (Figure 5(b)).

Carbonate represents the main cementing material in the phosphorites of Abu Had area and recorded mainly in phosphate samples of upper member samples 17, 22, 23 and 26 (Figure 5(a,c)). Silica cement is recorded in phosphate samples of lower and middle member samples 2, 5, 12 and 20 in amorphous form and represented by chalcedony (Figure 5(b)).

5. Mineralogy

The XRD data of bulk samples obtained from the studied phosphate samples recorded the presence of hydroxylapatite as the principal phosphate mineral in phosphate samples representing the three members of Duwi Formation in the study area (Figures 6–8). It provides the mineral content of organically formed bones and teeth. Generally, the apatite lattice is an open lattice which allows a greet number of isomorphous substitution. For this reason, a great number of varieties of natural phosphate mineral are known. It is identified at reflections 2.79, 2.28 and 1.87 that coincide with PDF_2 card no. (3–0747).

The non-phosphate minerals identified in the studied phosphate samples include calcite, quartz, gypsum and anhydrite (Figures 6–8).

Calcite mineral is the major non-phosphate mineral constituent of the most studied phosphate samples. Its occurrence in the studied phosphate samples affected by the occurrence of hydroxylapatite and quartz minerals, where its occurrence increase with the increase of hydroxylapatite minerals and decrease of quartz mineral (Figures 6–8). As mentioned by petrographical studies, calcite is recorded as cement and occasionally replaces the phosphate minerals in the bioclastic allochemes. It is identified at reflections 3.03, 3.85 and 2.09 that coincide with PDF_2 card no. (072–1214).

Quartz mineral occurs as detrital grains and crystalline silica (chalcedony). Its charts show high distribution in the lower member phosphatic samples (Figure 6). The petrographic examination revealed the enrichment of silica cement and replacement of phosphate minerals and bone fragments by silica in the studied phosphorites. It is identified by reflections 3.34, 4.26 and 1.84 using PDF_2 card no. (085–0798).

Gypsum and anhydrite minerals are common in weathered phosphate rocks of the middle member of Duwi Formation (Figure 7) and phosphatic sandstone rocks of the lower member of Duwi Formation (Figure 6). These minerals occur as cementing material of flaky and fibrous crystals filling inter-granular pore spaces. Presence of gypsum in these samples is probably due to pyrite oxidation during the phosphatisation diagenetic process and deposition or during the cementation processes.

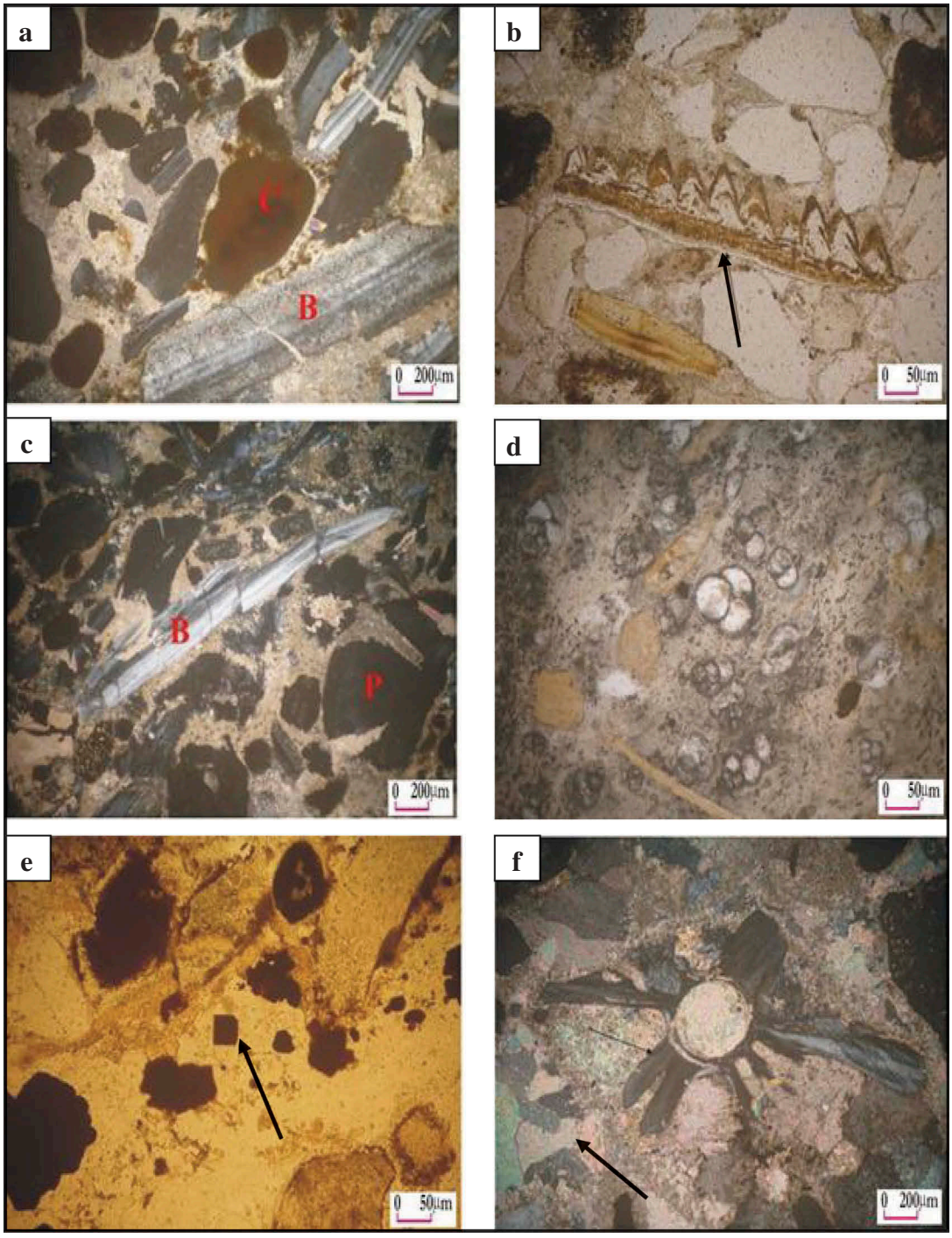

Figure 5. (a) Collophane grains (C) and bone fragments (B) embedded in carbonate cement (PPL. X20), (b) Jaw of fish (arrow) and quartz grains in silica cement (XPL. X40), (c) Phosphatic pellets (P) and bone fragment (B) embedded in carbonate cement (PPL. X20), (d) Plankton Foraminifera and bone fragments in carbonate cement (XPL. X40), (e) Pyrite cubes and quartz grains embedded in silica matrix (XPL. X40) and (f) Spinal vertebrae, calcite grains and bone fragments in carbonate cement (XPL. X40).

6. Ground gamma-ray spectrometric survey

In the present study, the spectrometric image maps (Figures 9–14) were prepared for showing the distribution of the three radioelements (K, U and Th) of Abu Had area and their geochemical ratios (eU/eTh, eU/K and eTh/K). The relationship between the radioelement distribution, different geologic units, and the main structure of Abu Had area was discussed and interpreted.

6.1. K (%) distribution map

Potassium distribution image map (Figure 9) shows that the potassium concentrations in the studied area ranging from 0.79% to 4.41%. The south part of the study area shows K content reaching 4.41% which associated with wadi sediments and Qusseir Formation. Meanwhile, phosphate beds of Duwi Formation possess low potassium concentrations less than 1%, associated

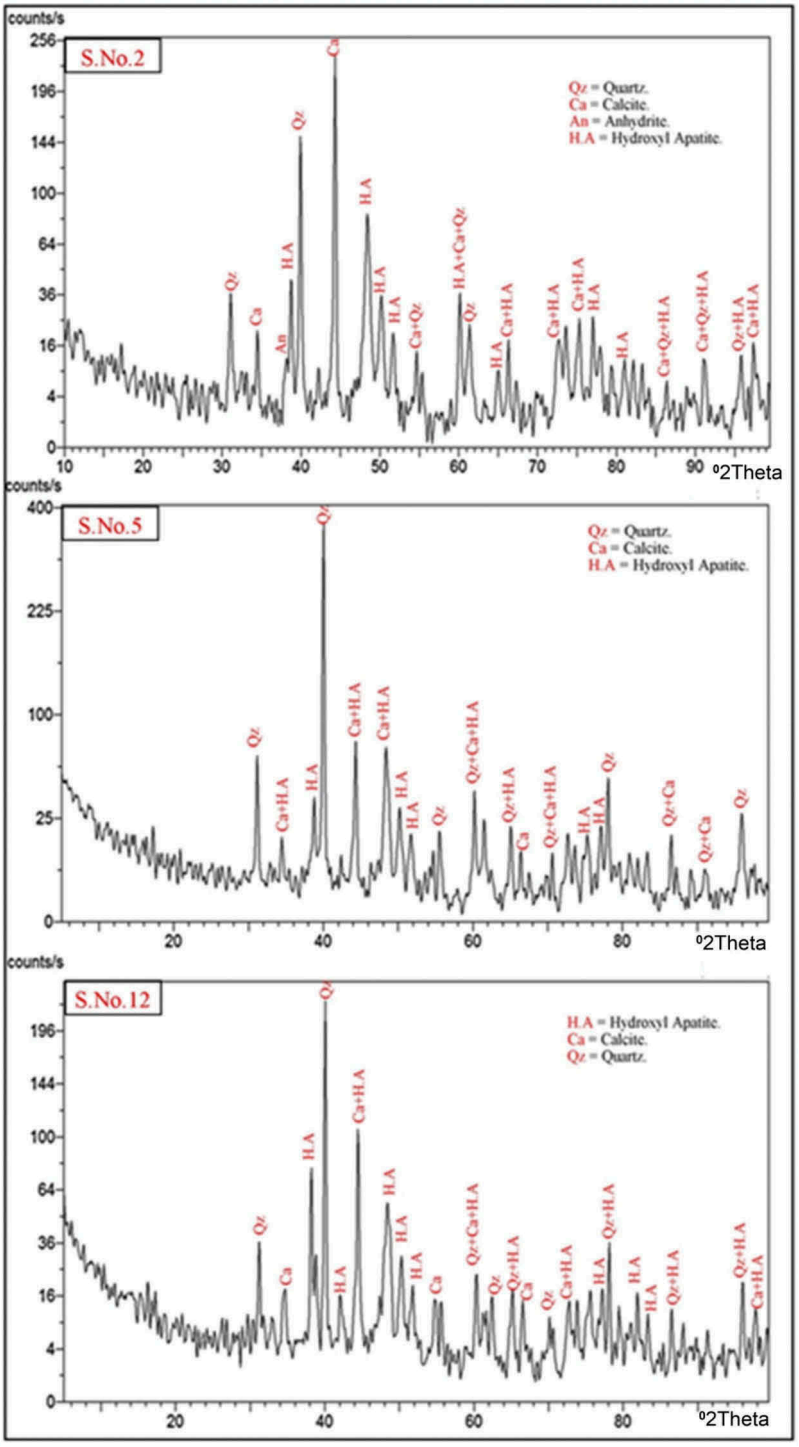

Figure 6. XRD pattern of phosphate samples from lower member of Duwi Formation at Abu Had area.

with central, northwest and southeast parts of the study area, trending in NW-SE direction.

6.2. eTh (ppm) distribution map

Equivalent thorium concentration of the studied area (Figure 10) ranges from 2.6 to 18 ppm with an average of about 9 ppm. The highest values of eTh are recorded in both the north-western part and the southern part which associating with Dakhla Formation and Qusseir Formation, respectively. Shale beds of Duwi Formation being present in the northern and central parts of the study area have eTh concentrations range from 4 to 9 ppm. Phosphate beds of Duwi Formation located in the southeastern and central parts of the studied area have low eTh concentrations range from 2.6 to 6 ppm.

6.3. eU (ppm) distribution map

Equivalent uranium concentrations in the Abu Had area range from 0.5 to 100 ppm with an average of about 38 ppm (Figure 11). Phosphate beds of Duwi Formation have high equivalent uranium concentrations range from

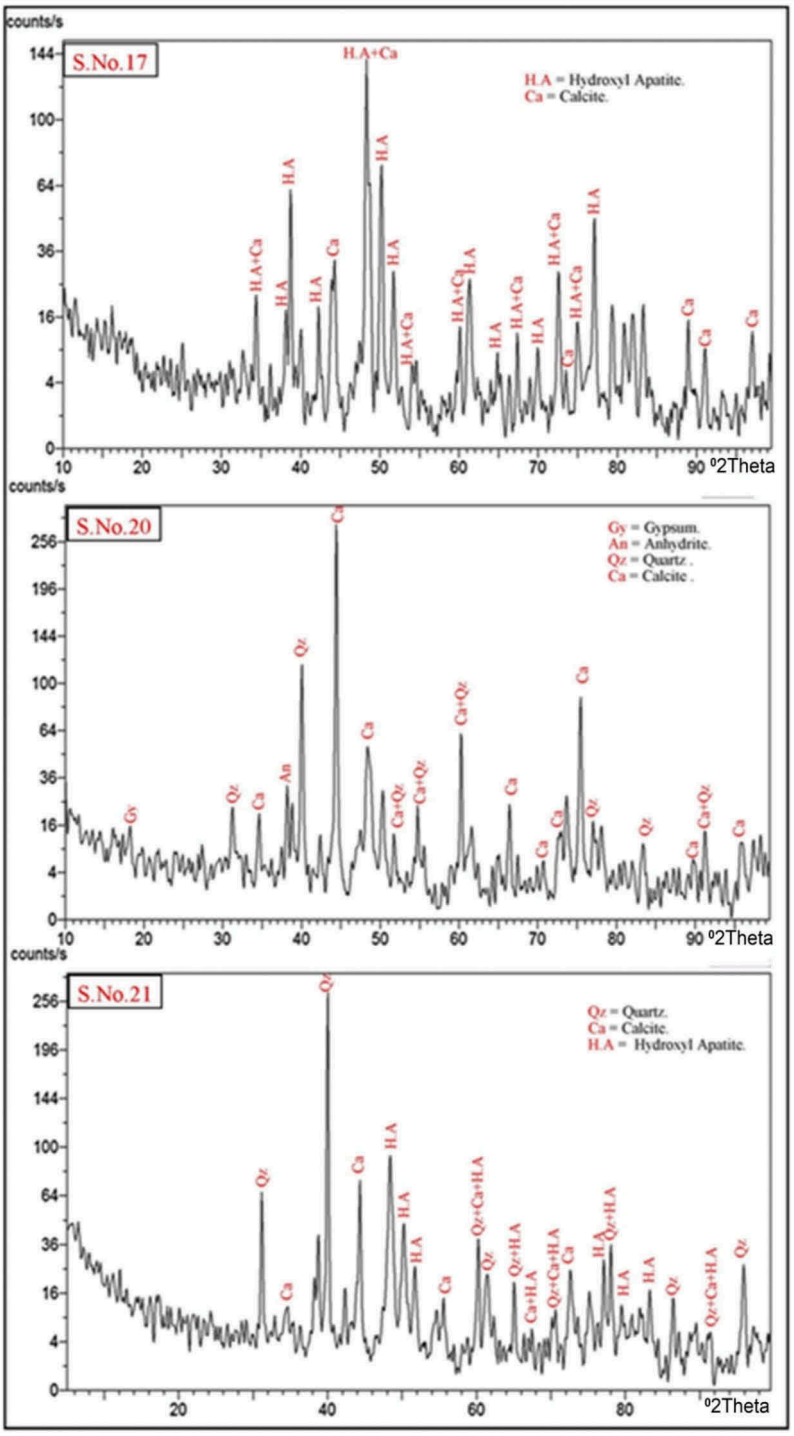

Figure 7. XRD pattern of phosphate samples from middle member of Duwi Formation at Abu Had area.

30 to 100 ppm. They are exposed in three localities (central, northwestern and southeastern parts of the study area). The uranium anomalies mostly elongated in NW-SE direction that related to the major structural trend; NW-SE strike-slip faults; of the studied area. Shale beds of Duwi Formation exposing in between phosphate layers and Dakhla Formation in northwestern parts of the study area show eU ranges from 15 to 28 ppm. Meanwhile, the northwestern part and central-eastern part of the study area are characterised by the lowest concentrations of eU range from 0.5 to 15 ppm. These parts are associated mainly with Qusseir Formation.

6.4. eU/eTh ratio image map description

eU/eTh ratio image map (Figure 12) shows that the eU/eTh ratio in Abu Had area ranges from 0.05 to 30.2. There are many eU/eTh anomalies reaching to 30.2 with NW-SE direction, due to high eU concentrations that associated with phosphatic beds of Duwi Formation. The shale beds of Duwi Formation occurring in central parts of the study area in between phosphate beds have eU/eTh ratio ranging from 5 to 19. Most parts of the study area show eU/eTh ratio range from 2 to 7 that are associated with Qusseir Formation and Dakhla Formation.

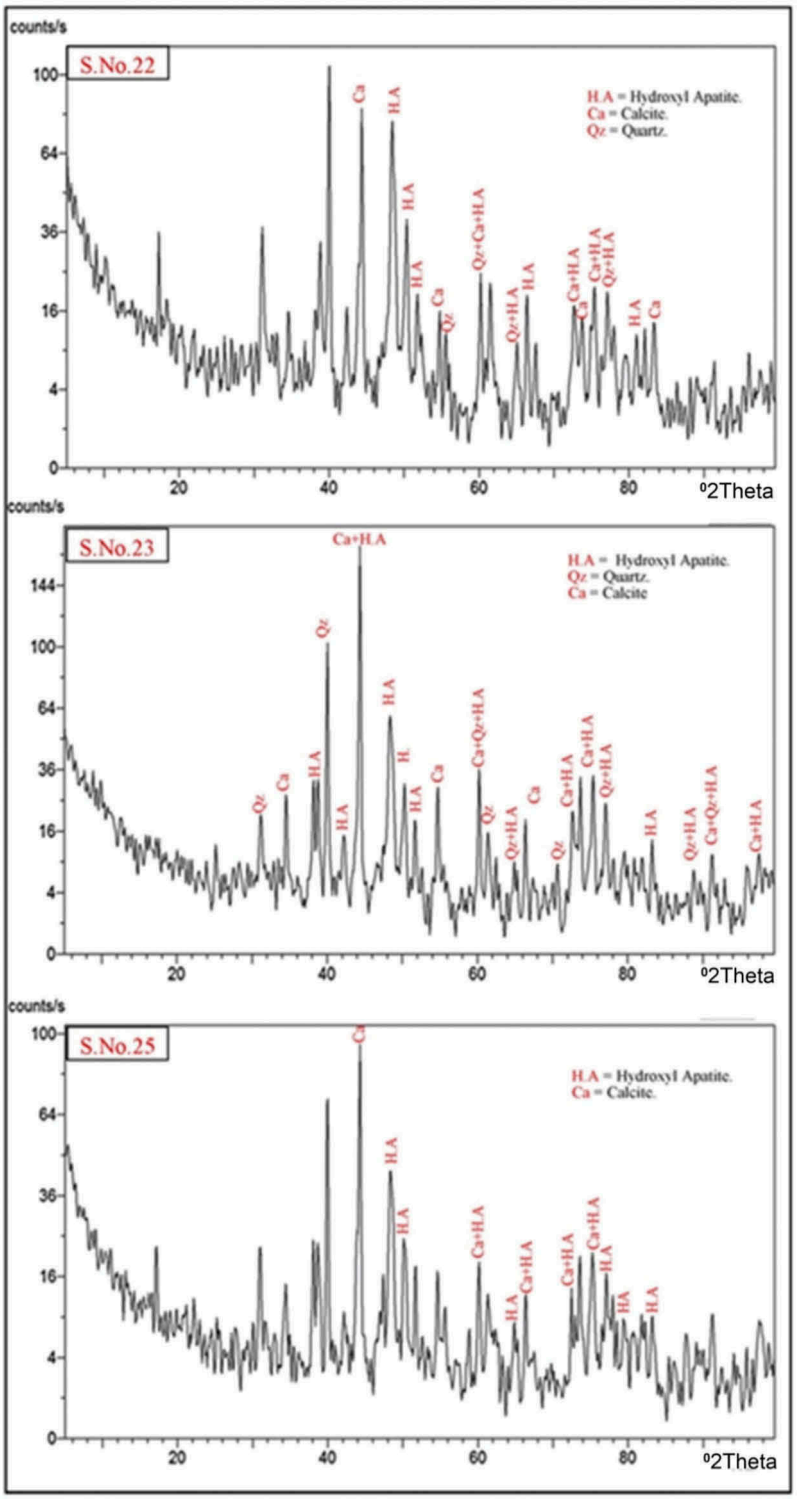

Figure 8. XRD pattern of phosphate samples from upper member of Duwi Formation at Abu Had area.

6.5. eU/K ratio image map description

eU/K ratio image map (Figure 13) shows that eU/K ratio in the area ranging from 1.1 to 149. The phosphate beds of Duwi Formation have the highest values ranging from 19 to 149, which represent three anomalies in the central part, northwest zone and southeast part of the study area. These three anomalies are elongated in NW-SE direction that controlled by the NW-SE strike-slip faults of the area. Shale beds of Duwi Formation exposed in central parts of the study area have eU/K ratio range from 1.75 to 94. Dakhla Formation and Qusseir Formation that exposed in the northwestern part and the southwestern parts of the study area, respectively, are characterised by the lowest eU/K ratio values (2 to 70).

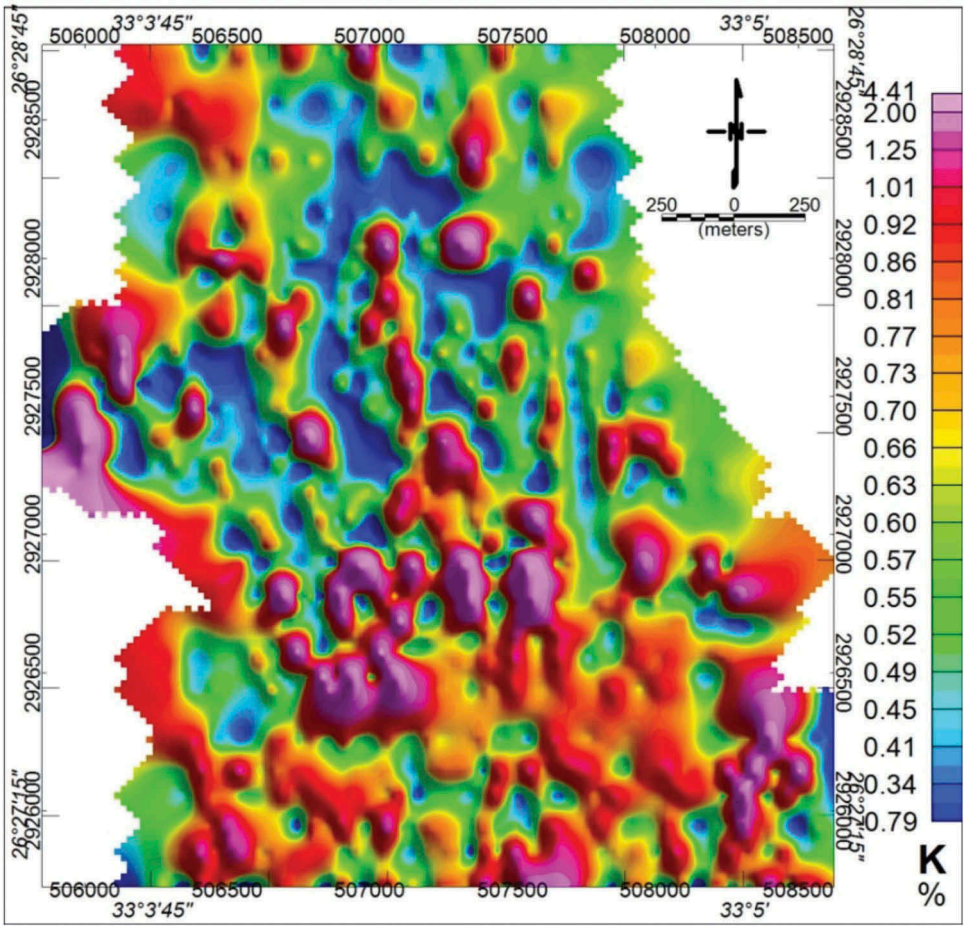

Figure 9. Ground K (%) image map of Abu Had area, Central Eastern Desert, Egypt.

6.6. eTh/K ratio image map description

eTh/K ratio image map (Figure 14) shows that its values range from 0.3 to 41.2. There are two main anomalies, first anomaly lies in southern parts and elongated from west to east direction that related to Qusseir Formation. The second anomaly lies in northwestern part of the study area which covered by Dakhla Formation. Shale beds of Duwi Formation exposing in between phosphate layers have small anomalies of eTh/K ratio reaching to 20 in the central-western part of the study area. Phosphate beds of Duwi Formation have the lowest eTh/K values range from 1 to 27.3, where the phosphate beds of the study area have the lowest values of both eTh and K.

7. Statistical analysis of the ground spectrometric data

The ground spectrometric data for different formations of Abu Had study area were subjected to statistical analysis explaining the relation between the radioactivity values and geological setting of the area (Table 1).

7.1. Qusseir formation

The range of radioactivity of this formation varies from 0.2% to 4% for K, from 1.3 to 20 ppm for eU and from 1.6 to 18 ppm for eTh. Meanwhile, eU/eTh ratio ranges from 0.17 to 764, eU/K ratio ranges from 1.1 to 67 and eTh/K ratio ranges from 1.82 to 35.5 (Table 1). The eU, eTh and eTh/K data have standardised skewness and kurtoses values lie inside the range of −2 to +2 which indicates symmetry of the data distribution and some significant normality for Qusseir Formation. The K, eU/K and eU/eTh data have standardised skewness and kurtoses values greater than +2 so, they have flatter or more peaked distribution shape than the normal distribution (Table 1).

7.2. Phosphate beds of Duwi formation

It represents the highest uranium content in Abu Had area. The range of radioactivity of these beds varies from 0.2% to 2.3% for K, 20 to 100 ppm for eU and 1 to 11.9 ppm for eTh. Meanwhile, eU/eTh ratio ranges from 2.27 to 31.87, eU/K ratio ranges from 19.17 to 152.6 and eTh/K ratio ranges from 1 to 27.3 (Table 1).

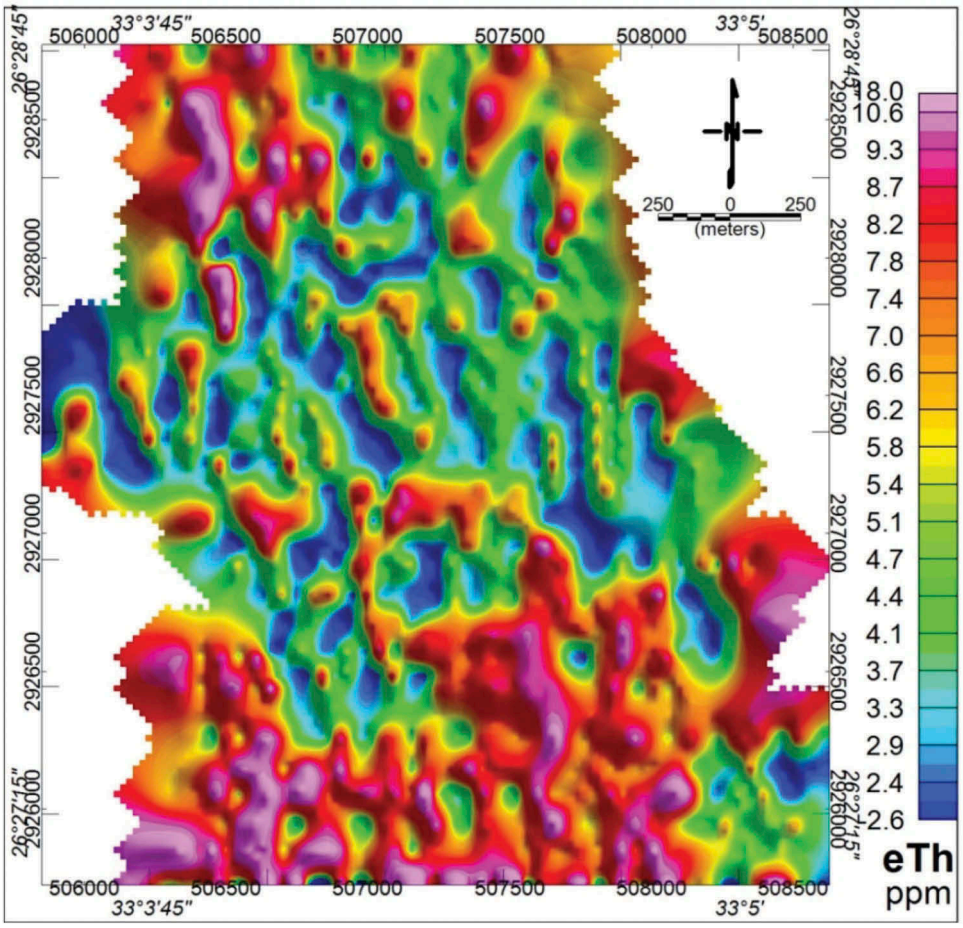

Figure 10. Ground eTh (ppm) image map of Abu Had area, Central Eastern Desert, Egypt.

The eU, eTh, eU/eTh, eU/K and eTh/K data have standardised skewness and kurtosis values lie inside the range of –2 to +2 which indicate symmetry of the data distribution and indicate some significant normality in these data. The K% data have standardised skewness and kurtosis values lie greater than +2 so they are asymmetric data and have flatter or more peaked distribution shape than the normal distribution (Table 1).

7.3. Shale beds of Duwi formation

The range of radioactivity of these beds of Duwi Formation variesfrom 0.2% to 5.1% for K, 0.5 to 20 ppm for eU and 0.5 to 15 ppm for eTh. Meanwhile, eU/eTh ratio ranges from 0.05 to 19.5, eU/K ratio ranges from 1.75 to 94 and eTh/K ratio ranges from 0.3 to 46.5 (Table 1). The eU, eTh and eU/K data have standardised skewness and kurtosis values lie inside the range of –2 to +2 which indicate symmetry of the data distribution and significant normality. The K, eU/eTh and eTh/K have standardised skewness and kurtosis values greater than +2 so they are asymmetric data and have flatter or more peaked distribution shape than the normal distribution (Table 1).

7.4. Dakhla formation

The range of radioactivity of this formation varies from 0.2% to 3.8% for K, 4.1 to 22.7 ppm for eU and 0.6 to 15 ppm for eTh. Meanwhile, eU/eTh ratio ranges from 0.59 to 15.17, eU/K ratio ranges from 2.73 to 70 and eTh/K ratio ranges from 1.44 to 20.25 (Table 1). The K, eU, eTh, eU/K and eTh/K data have standardised skewness and kurtosis values which lie inside the range of –2 to +2 which indicate symmetry of the data distribution and a normal distribution shape. The eU/eTh data have standardised skewness and kurtosis values greater than +2 so they are asymmetric data and have flatter or more peaked distribution shape than the normal distribution due to the relative enrichment of eU compared to eTh (Table 1).

7.5. Wadi sediments

The range of radioactivity of this formation varies from 0.3% to 1.5% for K, 3 to 28.6 ppm for eU and 1.2 to 11.4 ppm for eTh. Meanwhile, eU/eTh ratio ranges from 0.35 to 23.8, eU/K ratio from 2 to 57.2 and eTh/K ratio from 2.4 to 21.8 (Table 1). The K, eU, eTh, eU/K and eTh/K have standardised skewness and

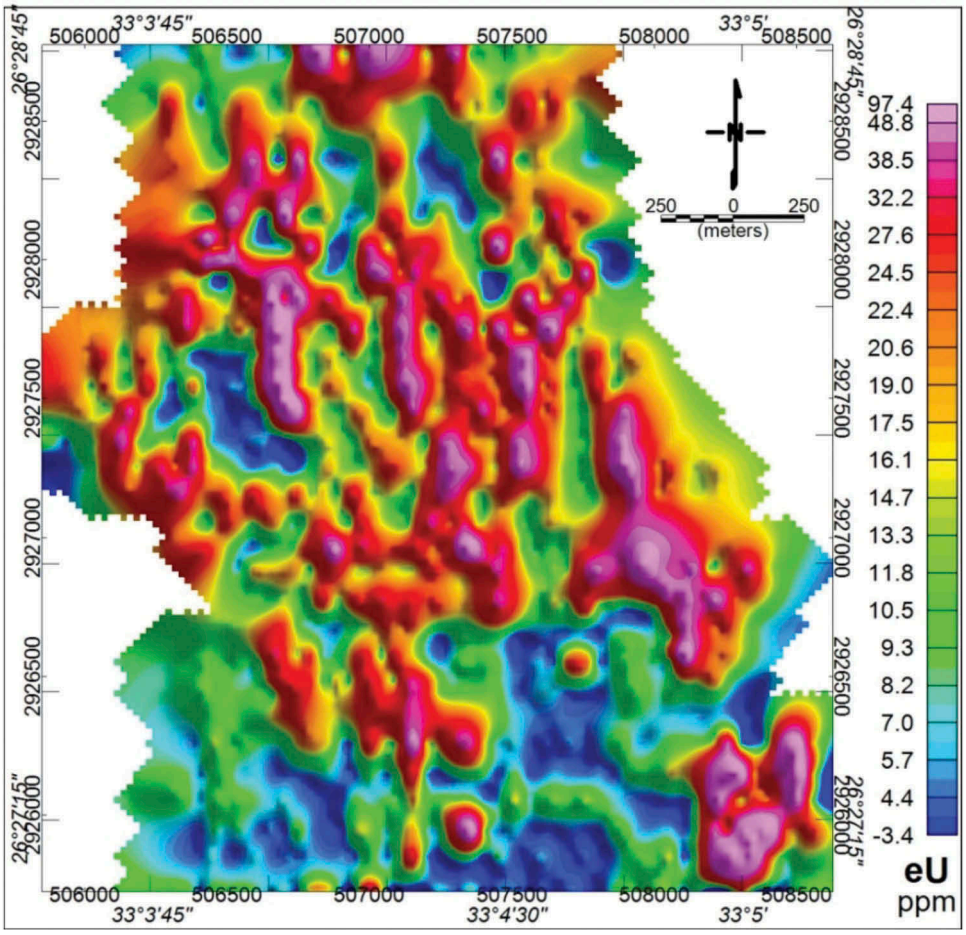

Figure 11. Ground eU (ppm) image map of Abu Had area, Central Eastern Desert, Egypt.

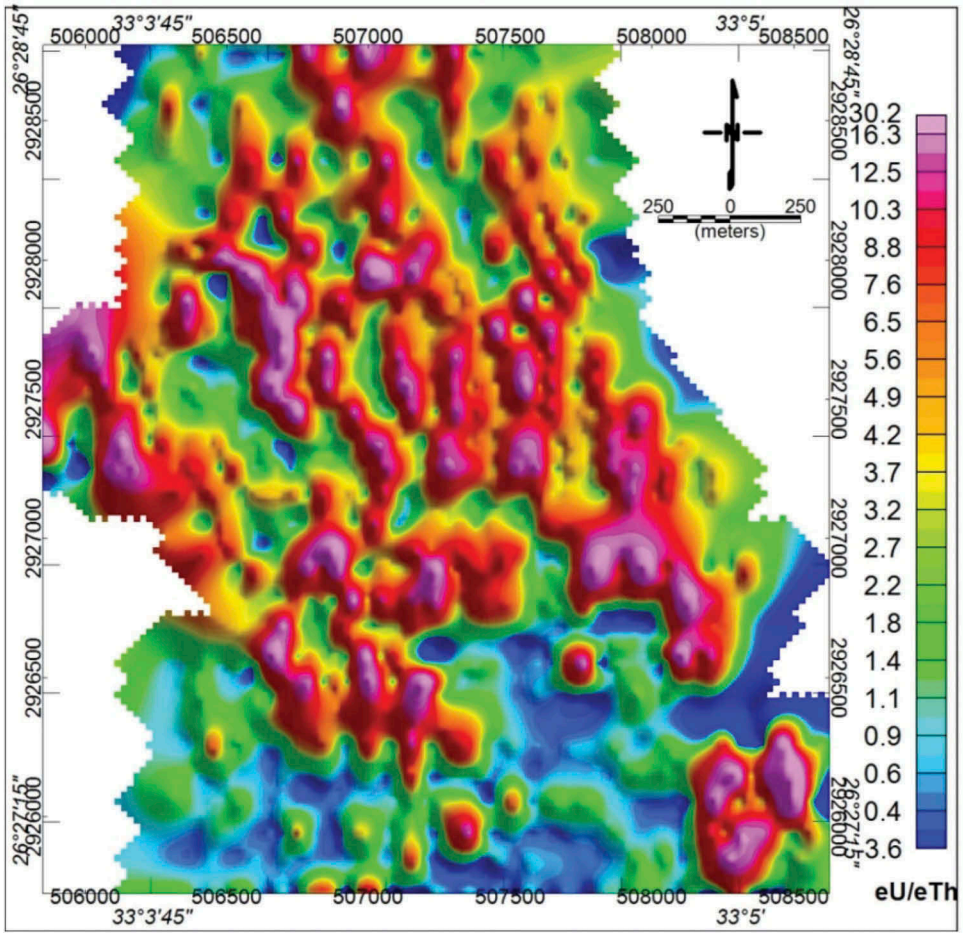

Figure 12. Ground eU/eTh ratio image map of Abu Had area, Central Eastern Desert, Egypt.

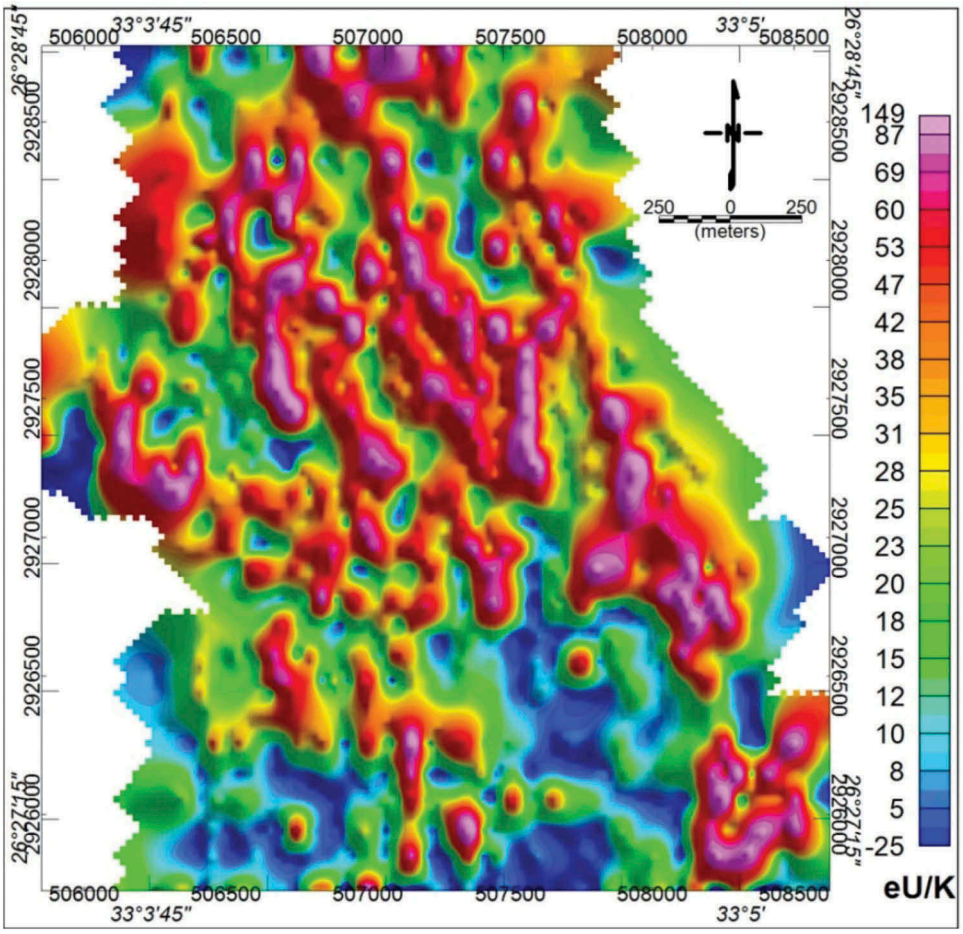

Figure 13. Ground eU/K ratio image map of Abu Had area, Central Eastern Desert, Egypt.

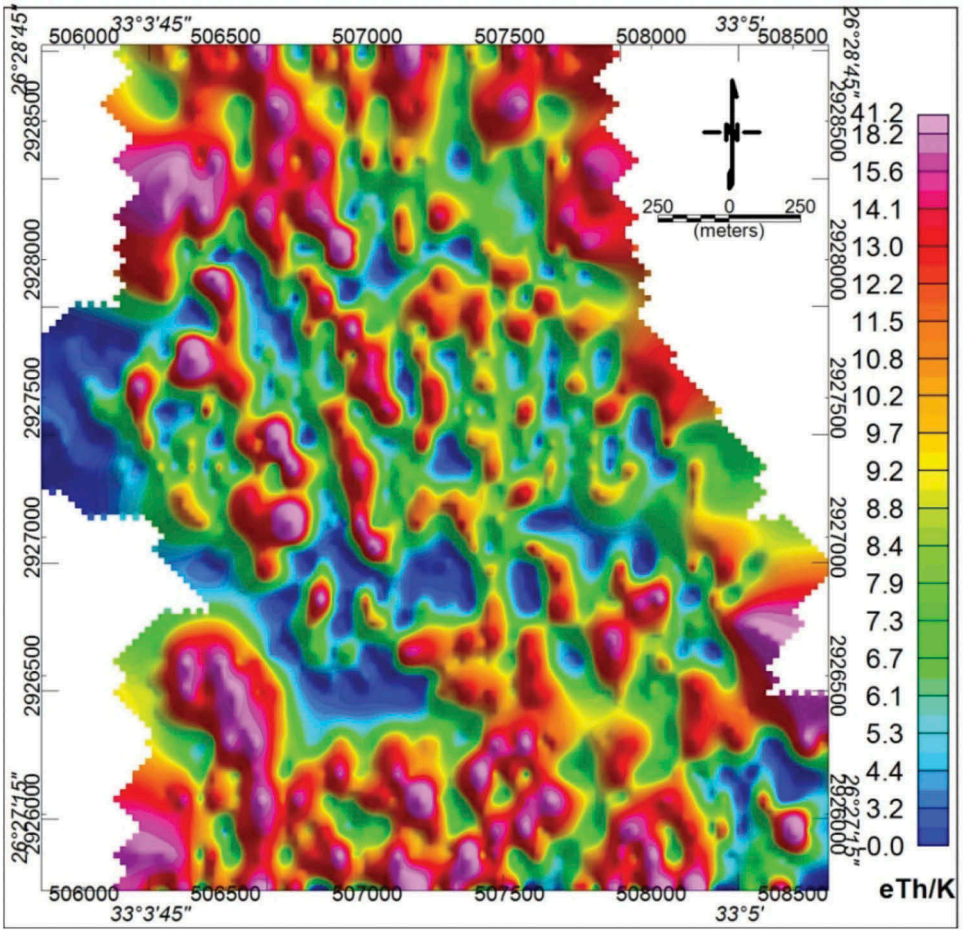

Figure 14. Ground eTh/K ratio image map of Abu Had area, Central Eastern Desert, Egypt.

Table 1. Statistical summary of ground spectrometric data of various radioelements and their ratios in the Abu Had area.

				K%				
Rock Types	N	Min.	Max.	Range	$\bar{X}$ (Mean)	SD	Skew.	Kurt.
Qusseir Fm.	169	0.2	4	3.8	0.82	0.47	3.61	19.09
Ph. of Duwi Fm.	318	0.2	2.3	2.1	0.66	0.36	2.06	5.27
Sh. of Duwi Fm.	437	0.2	5.1	4.9	0.77	0.73	3.29	11.56
Dakhla Fm.	21	0.2	3.8	3.6	1.12	1.08	1.46	0.57
W. Sediments	58	0.3	1.5	1.2	0.72	0.24	0.37	0.59
Total Types	1003	0.2	5.1	4.9	0.75	0.59	3.63	16.20
eU (ppm)								
Qusseir Fm.	169	1.3	20	18.7	7.75	3.70	0.68	0.12
Ph. of Duwi Fm.	318	20	100	80	37.75	15.77	0.99	0.33
Sh. of Duwi Fm.	437	0.5	20	19.5	11.17	4.92	0.02	−1.14
Dakhla Fm.	21	4.1	22.7	18.6	12.42	5.09	0.28	−0.54
W. Sediments	58	3	28.6	25.6	10.25	5.85	1.10	0.92
Total Types	1003	0.5	100	99.5	19.12	16.24	1.64	2.52
eTh (ppm)								
Qusseir Fm.	169	1.6	18	16.4	8.25	2.79	0.14	0.42
Ph. of Duwi Fm.	318	1	11.9	10.9	3.97	1.88	0.86	0.86
Sh. of Duwi Fm.	437	0.5	15	14.5	5.84	2.92	0.37	−0.38
Dakhla Fm.	21	0.6	15	14.4	7.14	3.79	0.42	−0.26
W. Sediments	58	1.2	11.4	10.2	7.13	2.22	−0.85	0.76
Total Types	1003	0.5	18	17.5	5.76	2.99	0.54	−0.12
eU/eTh ratio								
Qusseir Fm.	169	0.17	7.6	7.47	1.22	1.25	3.01	10.81
Ph. of Duwi Fm.	318	2.27	31.9	29.60	11.58	6.25	0.95	0.59
Sh. of Duwi Fm.	437	0.05	19.5	19.45	2.78	2.55	2.52	9.16
Dakhla Fm.	21	0.59	15.2	14.57	2.96	3.28	2.47	6.33
W. Sediments	58	0.35	23.8	23.48	2.11	3.40	4.95	27.11
Total Types	1003	0.05	31.9	31.82	5.27	5.93	1.76	3.00
eU/K ratio								
Qusseir Fm.	169	1.08	67	65.92	12.54	10.57	2.00	5.26
Ph. of Duwi Fm.	318	19.17	152.6	133.43	66.56	31.81	0.81	0.03
Sh. of Duwi Fm.	437	1.75	94	92.25	21.21	15.04	1.33	1.32
Dakhla Fm.	21	2.73	70	67.27	22.78	20.16	0.97	−0.38
W. Sediments	58	2.00	57.2	55.20	17.40	13.72	1.38	1.21
Total Types	1003	1.08	152.6	151.52	33.94	31.00	1.50	2.08
eTh/K ratio								
Qusseir Fm.	169	1.83	35.50	33.68	11.68	5.50	0.99	1.84
Ph. of Duwi Fm.	318	1.00	27.33	26.33	7.20	4.38	1.28	1.59
Sh. of Duwi Fm.	437	0.29	46.50	46.21	9.77	5.69	2.12	9.49
Dakhla Fm.	21	1.44	20.25	18.81	10.13	6.35	0.12	−1.40
W. Sediments	58	2.40	21.80	19.40	10.52	3.86	0.62	0.60
Total Types	1003	0.29	46.50	46.21	9.33	5.43	1.59	6.01

Table 2. Statistics of the annual effective dose rate (mSv/y) for Abu Had rock units.

Rock unit	N	Min.	Max.	$\bar{X}$ (Mean)	SD	skewness	kurtosis
Qusseir Fm.	169	0.051	0.224	0.107	0.026	1.01	2.9
Ph. of Duwi Fm.	318	0.135	0.843	0.325	0.127	1.11	0.72
Sh. of Duwi Fm.	437	0.018	0.265	0.128	0.044	0.073	−0.63
Dakhla Fm.	21	0.06	0.233	0.121	0.054	−0.47	−0.92
W. Sediments	58	2.40	0.211	0.14	0.044	1.07	0.35
Total Types	1003	0.018	0.843	0.187	0.123	1.76	3.2

kurtosis values lie inside the range of −2 to +2 which indicate symmetry and normality of the data distribution. The eU/eTh data have standardised skewness and kurtosis values greater than +2 so they are asymmetric data and have flatter or more peaked distribution shape than the normal distribution (Table 1).

The calculated standard deviations (SD) of all ground spectrometric data of the studied area are small compared to the adjacent arithmetic mean ($\bar{X}$) indicate a low dispersion of the data around the calculated mean value (Table 1).

8. Environmental assessments

Radiation dose is expressed in terms of energy received per unit weight. Different types of radiation have different penetrating power, and different parts of the body have different sensitivities to radiation. Effective dose is expressed in sievert (Sv) and usually reported per year. Dose assessment, therefore, requires knowledge of the type and amount of radiation as well as the biological sensitivity of the body part exposed.

The annual effective dose rate (mSv/y) can be estimated by using the following equation (United Nations Scientific Committee on the

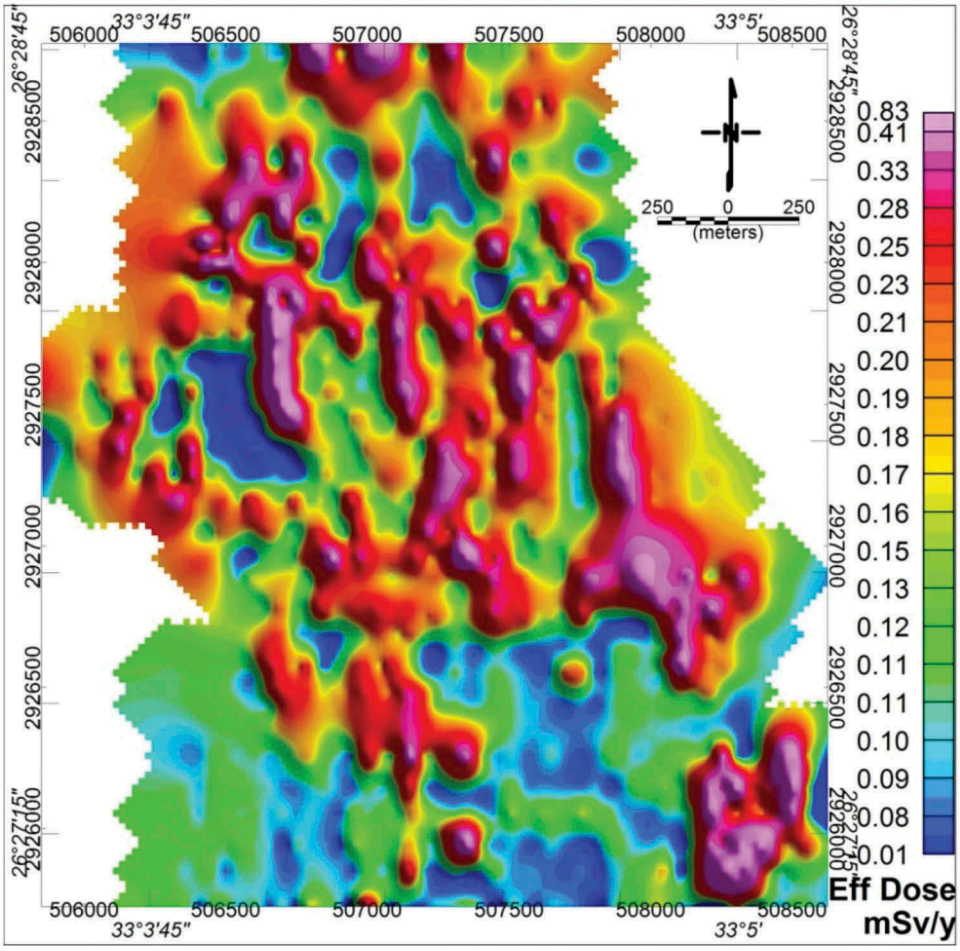

Figure 15. Ground annual effective dose map of Abu Had area, Central Eastern Desert, Egypt.

Effects of Atomic Radiation Report (UNSCEAR, 2000)): $\mathbf{E} = \mathbf{D_R} \times \mathbf{t} \times \mathbf{0.2} \times \mathbf{0.7} \times \mathbf{10^{-6}}$

where **E** is the annual effective dose rate (mSv/y), $\mathbf{D_R}$ is the dose rate (nSv/h), **t** is the exposure time. The effective dose rate (mSv/h) was calculated for 1 year (**t** = 8760 h), **0.7** Sv/Gy is the conversion coefficient from absorbed dose to effective dose and **0.2** is the fraction of time spent outdoors. In case of Abu Had area, the mean natural radiation dose rates received by members of the public from the ground gamma-radiation range from 0.018 to 0.843 mSv/y with an average 0.19 mSv/y (Table 2), where phosphate-bearing beds of Duwi Formation have annual dose rates range from 0.135 to 0.843 mSv/y with an average 0.33 mSv/y (Figure 15). These values remain in the safe side and less than the maximum permissible safe radiation dose rate which equals 1 mSv/y.

9. Conclusion

The aim of this work is to study the mineralogy of phosphatic rocks of Abu Had area and follow up the airborne uranium anomalies for the northern part of the study area by ground gamma-ray spectrometric survey. The study area is composed mainly of a simple sedimentary succession ranging from Upper Cretaceous to Quaternary age. The Duwi Formation in the study area conformably overlies the Qusseir Formation and underlies the Dakhla Formation. It is represented by three phosphorite members where the lower member is composed of yellowish-brown phosphate bands at weathered exposed surface, interbedded with thin blackish shale, chert lenses and calcareous clay stone bed, with an average 2 m in thickness. The middle member is composed of grey to black, papery shale, cross-bedded siltstone, marl, oyster bank and thin phosphatic layer with maximum thickness approximately 57 m. The upper member is composed of yellowish-brown phosphate with dolomitic lenses, black shale and capped with fossiliferous limestone bed, with an average thickness of 5.35 m. Petrographically, the studied thin sections of representative phosphate samples of study area are composed of phosphate particles include mudclasts represented by peloids (collophane grains), bioclasts (bone and teeth fragments), beside non-phosphate particles of quartz, calcite and pyrite embedded in silica, calcite, iron oxides or gypsum cement. X-ray diffraction results showed that hydroxylapatite is the only phosphate mineral composing the phosphorites of the studied samples; quartz, calcite and gypsum are also present in variable amounts. The spectrometric image maps were prepared and subjected to qualitative and quantitative

interpretation to determine radioactive anomalies and associated rocks. The spectrometric results showed that the study area has K values range from 0.2% to 4.4%, eTh values range from 0.5 to 18 ppm, and eU values range from 0.5 to 100 ppm. Qusseir Formation has the highest levels of both eTh and K in the study area up to 18 ppm and 4 %, respectively. Meanwhile, the phosphate-bearing beds of Duwi Formation have the highest values of eU reaching up to 100 ppm and lowest values of each eTh and K. These data showed that Abu Had area has uranium enrichment in the phosphatic beds. The annual effective dose rates of phosphate-bearing beds at Abu Had area range from 0.13 to 0.84 mSv/y with an average 0.32 mSv/y, which is less than the worldwide value of 1 mSv/y for the public exposure.

Disclosure Statement

No potential conflict of interest was reported by the authors.

References

Abbady AGE. 2004. Estimation of radiation hazard indices from sedimentary rocks in Upper Egypt, Technical note. Appl Radiat Isot. 60(1):111–114. doi:10.1016/j.apradiso.2003.09.012.

Abdu NMF. 2002. Distribution of uranium, thorium and rare earth elements in some Egyptian phosphorites. Precede 13th Symp. Phaner. Develop., Egypt. pp. 213–224.

Abou El-Anwar EA, Mekky HS, Abd El Rahim SH, Aita SK. 2016. Mineralogical, geochemical characteristics and origin of Late Cretaceous phosphorite in Duwi Formation (Gabal Duwi Mine). Red Sea region (Egypt): Egyptian Petroleum Research Institute.

Ahmed EA. 1983. Sedimentology and tectonic evolution of Wadi Qena area [Ph. D. Thesis]. Egypt: Assuit University.

Anderson H, Nash C. 1997. Integrated lithostructural mapping of the Rossing area, Namibia using high resolution aeromagnetic, radiometric, Landsat data and aerial photographs. Explorat Geophys. 28(1–2):185–191. doi:10.1071/EG997185.

Attia AM, Hulmy ME, Moursy AM. 1971. Composition and structure of phosphate deposits in A. R. E. Desert Inst Bull Cairo Egypt. 21(1):11–29.

Baioumy HM. 2007. Iron-phosphorous relationship in the iron and phosphorites ores of Egypt. Chemi Der Erde Geochem. 67(3):229–239. doi:10.1016/j.chemer.2004.10.002.

Egyptian Geological Survey and Mining Authority, (EGSMA). 2001. Geological map of Naj` el Bishariyah quadrangles, Egypt, scale 1: 100000. Geol. Surv. Cairo (Egypt).

Egyptian Geological Survey and Mining Authority, (EGSMA). 2002. Geological map of Jabal Shaib el Banat quadrangles, Egypt, scale 1: 100000. Geol. Surv. Cairo (Egypt).

El-Kammar AM. 1970. Mineralogical and geochemical studies on El-Hagarin El-Mossattaha phosphate, Sibaiya East [M. Sc. Thesis]. Egypt: Cairo University.

El-Kammar AM, Zayed MA, Amer SA. 1979. Rare earth of the Nile Valley phosphorites, Upper Egypt. Chem Geol. 24(1–2):69–81. doi:10.1016/0009-2541(79)90013-5.

El-Sawy EK, Bekhiet MH, Abd El-Motaal E, Orabi AA, Abd El Ghany MK. 2011. Geo-environmental studies on Wadi Qena, Eastern Desert, Egypt, by using remote sensing data and GIS. Al-Azhar Bull Sci. 22(Issue 2–D):33–60. doi:10.21608/absb.2011.7909.

Ford KL, Savard M, Dessau JC, Pellerin E. 2001. The role of gamma-ray spectrometry in radon risk evaluation: A case history from Oka, Quebec. Geosci Can. 28:2P.

Gaafar IM, Aboelkheir H, Bayoumi M. 2017. Integration of Gamma-Ray Spectrometric and Aster Data for Uranium Exploration in Qash Amer-El-Sela Area, Southeastern Desert, Egypt. Nucl Sci J. 6(1):17–33. doi:10.21608/nssj.2017.30771.

Gaafar IM, Ali KG, Meira MI. 2013. Integration of airborne and carborne gamma-ray spectrometric surveys, Wadi Elgidami area, Central Eastern Desert, Egypt. Egypt Geophys Soc J. 12:65–78.

Gaafar IM, Ali KG, Meira MI. 2014. Integration of airborne and carborne gamma-ray spectrometric surveys, Wadi El Gidami area, Central Eastern Desert, Egypt. Geophys Soc J. 12:65–78.

Gaafar IM, El-Shershaby A, Zeidan I, Sayed El-Ahll L. 2016. Natural radioactivity and radiation hazard assessment of phosphate mining, Quseir-Safaga area, Central Eastern Desert, Egypt. NRIAG J Astron Geophys. 5(1):160–172. doi:10.1016/j.nrjag.2016.02.002.

Germann K, Bock WD, Schorter T. 1984. Facies development of Upper Cretaceous phosphorites in Egypt: sedimentological and geochemical aspects. Berl Geowiss Abh A. 50:345–361.

Grasty RL, Shives RBK. 1997. Applications of gamma ray spectrometry to mineral exploration and geological mapping, a workshop presented at exploration 97: Fourth Decennial Conference on Mineral Exploration, Canada.

Hamama HH, Kassab AS. 1990. Upper Cretaceous ammonites of Duwi Formation in Gabal Abu Had and Wadi Hamama, Eastern Desert, Egypt. J Afr Earth Sci. 10 (3):453–464. doi:10.1016/0899-5362(90)90098-Y.

Hassaan MM, Zidan IH, Abd El-Moghny MW, Eldosoky HM, Elshazly MM. 2017. Uranium bearing phosphorite, West Sibaiya, Egypt: exploited mines characterization, and potential of surrounding areas. Curr Sci Int. 6:377–395.

Hermina MH. 1972. Review on the phosphate deposits of Egypt. 2nd Arab Conf. Mine, Res., Conf. Paper, Cairo. p. 109–149.

IAEA. 2010. Radioelement mapping, IAEA nuclear energy series. Vienna:International Atomic Energy Agency.

Lahti M, Jonsen DG, Multala J, Rainey MP. 2001Environmental applications of airborne radiometric surveys. Expanded Abstracts. 63th Annual Conference, European Association of Geoscientists and Engineers, Amsterdam.

McClellan GH. 1980. Mineralogy of the carbonate fluorapatite. J Geol Soc Lond. 137(6):675–681. doi:10.1144/gsjgs.137.6.0675.

Mohamed FY. 1994. Comparative study of the radioactivity and geochemistry of the Upper Cretaceous phosphate-bearing sediments in the Western and Eastern Sinai. Egypt: Fac. Sci., Cairo Univ..

Morsery AM. 1969. Comparative mineralogical studies of phosphate occurrences of Egypt [M. Sc. Thesis]. Egypt: Ain Shams University.

Notholt AG. 1985. Phosphorite resources in the Mediterranean (Tethyan) phosphatic province: A progress report. Sciences Geologiques. Memoire. 77:9–21.

Philobbos ER. 1969. Geology of the phosphate of the Nile Valley [Ph. D. Thesis]. Egypt: Assuit University.

United Nations Scientific Committee on the effects of Atomic Radiation Report (UNSCEAR). 2000. Sources and effects of ionizing radiation. United Nations Scientific Committee on the effects of atomic radiation sources to the general assembly with annexes, effects and risks of ionizing radiation. New York:United Nations Publications.

Zidan IH. 2013. Evaluation of phosphorite and Uranium in lower member, Duwi Formation at Kummer area south Esna, West Nile Valley, Egypt. J Sedimentoll Soc Egypt. 21:143–154.